Numerical Study of Granular Debris Flow Runup against Slit-dams by Discrete Element Method

Gordon G. D. Zhou[1&2], Junhan Du*[1&2], Dongri Song [1&2], Clarence E. Choi[3], H. S. Hu [1&2] and Chenghua Jiang[4]

1. Key Laboratory of Mountain Hazards and Earth Surface Process/Institute of Mountain Hazards and Environment, Chinese Academy of Sciences (CAS), Chengdu, China

2. University of Chinese Academy of Sciences, Beijing, China

3. Department of Civil Engineering, The University of Hong Kong, Pok Fu Lam, Hong Kong

4. Kunming Dongchuan Debris Flow Prevention and Control Institute, Kunming, China

*Corresponding author

Information of the authors

Corresponding author: Mr Junhan Du

Postgraduate student

E-mail: dujunhan17@mails.ucas.ac.cn

Co-author: Dr Gordon G. D. Zhou

Professor

E-mail: gordon@imde.ac.cn

Co-author: Dr Dongri Song

Associate Professor

E-mail: drsong@imde.ac.cn

Co-author: Dr Clarence E. Choi

Assistant Professor

E-mail: cechoi@hku.hk

Co-author: Mr H. S. Hu

Ph.D student

E-mail: huhongsen15@mails.ucas.edu.cn

Co-author: Ms Chenghua Jiang
Senior Engineer, Kunming Dongchuan Debris Flow Prevention and Control Institute, Kunming, China
E-mail: 282955245@qq.com

Numerical Study of Granular Debris Flow Runup against Slit-dams by Discrete Element Method

Abstract

Runup of granular debris flows against slit-dams on slopes is a complex process that involves deceleration, deposition and discharge. It is imperative to understand the runup mechanism and to predict the maximum runup height for the engineering design and hazard mitigation. However, the interaction between granular flows and slit dams, which significantly affects the runup height, is still not well understood.

In this study, an analytical model based on the momentum approach was derived to predict the runup heights of granular debris flows. A numerical investigation of granular debris flow impacting slit-dams using the discrete element method (DEM) was then conducted. The influence of the Froude number (N_{Fr}) and the relative post spacing (R) on runup height were studied.

This study illustrates that the analytical model based on the momentum approach can predict the runup heights well within a certain range of Froude numbers. There is a critical value of relative post spacing (R_C): within the critical value, the maximum runup height is insensitive to the relative post spacing; once R exceeds the critical value, the maximum runup height decreases rapidly as the relative post spacing increases.

Keywords: Granular debris flow; slit-dam; soil/structure interaction; runup height

1. Introduction

Granular debris flows comprise a wide range of particle sizes (Jakob et al. 2005), surging down slopes in response to gravity (Iverson et al. 1997). Due to the high mobility and the large volume of material (Shen et al. 2018), granular debris flows can result in disastrous consequences to human lives and facilities downstream (Hungr et al. 1984).

To mitigate such destructive hazards, slit-structures such as slit-dams (Watanabe et al. 1980; Armanini et al. 2001; Piton & Recking 2015a; Marchelli et al. 2019; Zhou et al. 2019) and baffle arrays (Choi et al. 2014a; Law et al. 2015) are often strategically installed along the predicted flow path. Such structures, comprising rigid planes (hereafter referred to as 'posts') and openings (referred to throughout as 'slits'), can dissipate flow energy, thereby arresting flows (Choi et al. 2014a; Zhou et al. 2019).

Granular debris flows impact rigid barriers and transfers momentum vertically into runup, potentially overtopping obstacles (Hákonardóttir 2003; Ng et al. 2016). Design of engineering countermeasures requires estimates of runup height to prevent overtopping (Kwan 2012; Choi et al. 2016; Ng et al. 2017). However, existing physically-based debris flow models may be unable to output the maximum runup heights accurately (Choi et al. 2015b; Iverson et al. 2016), given the complexity of the problem.

Multiple analytical models have been proposed to predict the maximum runup heights of granular avalanches/flows against rigid barriers (Hungr & McClung 1987; Chu et al. 1995; Mancarella & Hungr 2010). Nevertheless, there are two commonly adopted approaches for predicting debris flow runup height in practice (GEO 2012) – the energy approach (Armanini et al. 2011; Kwan 2012) and the momentum approach proposed by Hákonardóttir (2003) and Jóhannesson et al. (2009). The energy approach (Armanini et al. 2011; Kwan, 2012) is given as follows:

$$\frac{h_f}{h_i} = 1 + \frac{u^2}{2gh_i} \quad (1)$$

where h_f is the runup height, h_i is the height of incoming flow, u is the incoming flow velocity, and g is the acceleration due to gravity.

Another commonly adopted approach proposed by Jóhannesson et al. (2009) is based on conservation of mass and momentum:

$$\frac{\rho_f}{\rho_i}\left(\frac{h_f}{h_i}\right)^2 - \frac{h_f}{h_i} + \left(\frac{\rho_f h_f}{\rho_i h_i}\right)^{-1} - 1 - 2N_{Fr}^2 = 0 \quad (2)$$

where ρ_f is the density of the flow after runup and ρ_i is the density of the incoming flow. N_{Fr} is the Froude number of the incoming flow, indicating the ratio of inertial forces to gravitational forces. Subcritical and supercritical flow conditions are characterized with Froude numbers less than and greater than unity, respectively (Choi et al. 2015a; Ng et al. 2016).

For check dams (i.e. with no slit), it was found that the analytical approach proposed by Johannesson et al. (2009) can capture the pileup height for granular materials well. This is because the compression of granular flow material, as well as the pileup mechanism characteristic of granular materials, are explicitly accounted for (Choi et al. 2015b). In contrast, the energy approach is more appropriate for water, for which there is little energy dissipation, and which primarily undergoes runup since water has no shear strength, pileup cannot occur.

It is noted that both energy and momentum approaches (Jóhannesson et al. 2009; Armanini et al. 2011; Kwan 2012) were derived assuming that the barrier is closed (i.e. without any openings) so that no flow material can discharge. However, for the case of a slit-dam, flow-structure interaction is more complicated. Runup of flows against slit-dams is a complex process that involves a combination of flow deceleration, redirection and downstream discharge (Piton & Recking 2015a, 2015b). Unlike check dams, slit-dams usually have one or more slits to: (i) reduce the flow peak discharge (compared to open channel flow); and (ii) to dissipate kinetic energy (Choi et al. 2016). The model proposed by Armanini (2001) is able to predict the

deposition height of granular materials deposited by a continuously flowing stream that passes a slit-dam:

$$\frac{h_f}{h_i} = \frac{3}{2}\left(N_{Fr}\frac{w}{b}\right)^{\frac{2}{3}} - \frac{N_{Fr}^2}{2}\left\{1 - \left[1 - \frac{2}{3}\left(N_{Fr}\frac{w}{b}\right)^{-\frac{2}{3}}\right]^2\right\} \quad (3)$$

where w is the channel width and b is the slit size. However, this approach is only validated for flows with a solid fraction of up to 0·01 (Choi et al. 2016), which is substantially lower than the typical solid fraction for granular debris flows, around 0.6 (Denlinger & Iverson 2001).

In this study, an analytical model based on the momentum approach was derived to predict the runup heights of granular debris flows against slit-dams. Furthermore, the interaction between granular debris flows and slit-dams was studied numerically using the Discrete Element Method (DEM) (Cundall & Strack 1976; Teufelsbauer et al. 2009). Investigations of granular debris flows with varying Froude conditions (N_{Fr}) impacting slit-dams with different relative post spacings (b/d) were carried out. Runup heights determined using the analytical models were compared with the numerical and reported experimental results. The influence of flow regime and the relative post spacing on the runup height of granular debris flow was investigated.

2. Analytical model

To predict the runup heights of granular debris flows against slit-dams, a depth-averaged continuum model derived from assumptions similar to that of the momentum approach (Hákonardóttir 2003; Jóhannesson et al. 2009; Iverson et al. 2016) has been developed here. This analytical model is based on shock theory (Gray et al. 2003; Hákonardóttir 2003; Jóhannesson et al. 2009; Faug 2015; Iverson et al. 2016; Albaba et al. 2018). It assumes that the flow impinging on an obstacle is a one-dimensional dynamic problem which can be interpreted by the development of a shock. In this process, a shock (or shock wave), at which there are sudden jumps in the velocity, density and height, develops immediately and travels upstream when a

steady flow encounters a vertical obstacle. The incoming flow is assumed to be continuous, steady, uniform, compressible and insensitive to the backwater effect, and the flow channel is horizontal (cf. Iverson et al. 2016).

Fig. 1(a) shows a simplified sketch of a shock for granular debris flow against a check dam (a side view and a plan view). A shock develops and travels upstream with depth-invariant velocity u, height h, and bulk density ρ, while a granular dead zone forms between the shock and the dam. The conservation of mass and momentum across the shock travelling at speed *s* can be expressed as (cf. Jóhannesson et al. 2009; Iverson et al. 2016):

$$\rho_0 h_0(u_0 + s) = \rho_1 h_1(u_1 + s) \tag{4}$$

$$\rho_0 h_0 u_0(u_0 + s) + \int_0^{h_0} \sigma_{0_{xx}}\,\mathrm{dz} = \rho_1 h_1 u_1(u_1 + s) + \int_0^{h_1} \sigma_{1_{xx}}\,\mathrm{dz} \tag{5}$$

where subscript 0 denotes properties of the flow upstream of the shock, subscript 1 denotes properties of the flow downstream from the shock, σ_{xx} denotes the longitudinal normal stress.

As for the case of a slit-dam (Fig. 1(b)), a more complex process is involved which includes a combination of flow deceleration, redirection and downstream discharge. A shock develops and travels upstream at speed *s* as the incoming flow encounters the slit-dam. Due to regulation of the slit-dam, different from the check dam case, downstream flow from the shock transforms into two types: (*i*) one retards and deposits with speed u_1, forming a granular dead zone between the shock and the dam, which is similar to the check dam case; (*ii*) another propagates downstream with speed u_2 and then passes through the slit. The conservation of mass and momentum across the shock travelling at speed *s* can be expressed as:

$$\rho_0 h_0(u_0 + s) = (1 - B)[\rho_1 h_1(u_1 + s)] + B[\rho_2 h_2(u_2 + s)] \tag{6}$$

$$\begin{aligned}\rho_0 h_0 u_0(u_0 + s) + \int_0^{h_0} \sigma_{0_{xx}}\,\mathrm{dz} = (1 - B)\left[\rho_1 h_1 u_1(u_1 + s) + \int_0^{h_1} \sigma_{1_{xx}}\,\mathrm{dz}\right] \\ + B\left[\rho_2 h_2 u_2(u_2 + s) + \int_0^{h_2} \sigma_{1_{xx}}\,\mathrm{dz}\right]\end{aligned} \tag{7}$$

where subscript 0 denotes properties of the flow upstream of the shock, subscript 1 denotes properties of the (*i*) retarding flow downstream of the shock while 2 denotes properties of the (*ii*) outgoing flow downstream of the shock. B ($B = b/w$, where b is the width of spacing between posts and w is the width of channel) is the transverse blockage of the slit-dam. σ_{xx} is the longitudinal normal stress. Using of an assumption routinely employed in soil mechanics (Lambe and Whitman, 1979), σ_{xx} can be expressed as:

$$\sigma_{xx} = k\sigma_{zz} = k\rho g(h - z) \tag{8}$$

where k is the longitudinal pressure coefficient, which denotes the ratio of longitudinal to vertical normal stress σ_{zz}. The k values of typical frictional debris roughly range from 0.2 to 5, depending on whether deformation occurs in an extensional or compressional mode (Iverson and Denlinger, 2001). It was found that in the momentum approach, the assumption k = 1 yields good predictions of runup heights of debris flows and it can even be used in more sophisticated runup models (Iverson et al. 2016).

Considerable simplifications of (6) and (7) can be obtained by introducing a reasonable assumption that the two types flows downstream from the shock have the same density and height such that ρ_1 and h_1 are equal to ρ_2 and h_2, respectively. In this case, the mass jump condition (6) reduces to

$$s = \frac{\rho_0 h_0 u_0 + B\rho_1 h_1 (u_1 - u_2) - \rho_1 h_1 u_1}{\rho_1 h_1 - \rho_0 h_0} \tag{9}$$

Substitution of (8) in (7), and subsequent evaluation of the integrals for the momentum jump condition (7) yields

$$\rho_0 h_0 u_0 (u_0 + s) - B[\rho_1 h_1 u_2 (u_2 + s)] - (1 - B)[\rho_1 h_1 u_1 (u_1 + s)] - \frac{1}{2} kg\left(\rho_1 {h_1}^2 - \rho_0 {h_0}^2\right) = 0 \tag{10}$$

Downstream flow from the shock, the retarding flow deposits with speed u_1, forming a granular dead zone between the shock then the velocity u_1 can be supposed to be equal to 0. For the outgoing flow, the flow rheology between the shock and the slit dam is very complex with strong flow curvatures, flow redirection and formation of dead zones in the corners. In want of a detailed theory for this region, we

propose to consider an empirical linear relation between the outgoing velocity u_2 and the velocity u_0 of the incoming flow:

$$u_2 = \alpha u_0 \tag{11}$$

By combination of (9) and (11), momentum jump condition (10) reduces to

$$Fr_0{}^2[1 - 2B\alpha + B\alpha^2 - AB\alpha^2 + AB^2\alpha^2] - \frac{1}{2}k\left[A\frac{h_1}{h_0} - \frac{h_1}{h_0} - 1 + A^{-1}\right] = 0 \tag{12}$$

where $Fr_0 = u_0/\sqrt{gh_0}$, indicates the bulk characteristics of the incoming flow. The term A, which indicates the jump in density and height between the flows upstream and downstream of the shock, can be defined as follows:

$$A = \frac{\rho_1}{\rho_0}\frac{h_1}{h_0} \tag{13}$$

Equation (12) yields a runup formula based on momentum approach and it takes not only the upstream Froude conditions (N_{Fr}) but also the slit size (B) into consideration. For physically relevant parameter values (ρ_1/ρ_0~1), Eq. (12) has three real roots, but only one of these roots has physical relevance by virtue of being positive and satisfying the jump condition requirement that $h_1 > h_0$ (cf. Iverson et al. 2016).

Considering two extreme cases that the dam is completely closed ($B = 0$) or open ($B = 1$), the boundary conditions of (12) can be expressed as

$$\begin{aligned} &if\ \mathrm{B} = 0,\ \ u_2 = 0 \ \rightarrow\ \alpha = 0 \\ &if\ B = 1,\ \ u_2 = u_0 \ \rightarrow\ \alpha = 1 \end{aligned} \tag{14}$$

Based on the boundary condition, α can be assumed as a function of B:

$$\alpha = f(B) \tag{15}$$

An explicit expression of (14) can be obtained by introducing an exponential form which can meet the boundary conditions in Eq. (13)

$$\alpha = B^e \tag{16}$$

where e is an empirical coefficient.

Finally, substituting (15) into (12), the solutions of the runup formula can be obtained. Therefore, the runup height of granular debris flows against slit-dams can be predicted if the Froude number of the incoming flows and the geometry of the

slit-dams are known a priori.

3. Numerical model setup

The 3-D particulate flow code EDEM (TranscenData, 2007) is adopted to simulate the dynamics of granular flow in this study. In the DEM, contact forces and displacements of a stressed assembly of particles are found by tracing the movement of individual particles (Choi et al. 2014b). Compared to physical model tests, numerical simulations have a better capacity for capturing particle movements and interactions with structures (Zhou et al. 2013; Chen et al. 2019).

Slit-dams are usually comprised of a series of equally-spaced rigid posts (Marchelli et al. 2019; Zhou et al. 2019). The spacing and the number of posts can be varied depending on the engineering design adopted. In this study, the interaction between granular debris flows and slit-dams is studied by choosing a section which spans two adjacent posts since the processes which occur in the rest of the sections do not vary significantly with time. Fig. 2 shows the numerical model setup. The channel inclination θ is fixed at 20 ° and gravitational acceleration g (9.81 m/s^2) acts downwards, along the vertical direction. Planar rigid geometry is constructed to model the channel bed and the slit-dam. The sidewalls adopt periodic boundary conditions (PBC) (Rapaport et al. 2004) which are applied along the flow direction and spans the width of the channel (0.2m). The PBC is required to eliminate the unrealistic particle arrangement at the wall boundary caused by the constraint of particle sizes in discrete element simulations (Rapaport et al. 2004). A slit-dam with rigid barriers and an adjustable spacing b is positioned downstream of the flows. The rigid barriers are set to be 2 m in height, perpendicular to the base of the channel. This is high enough to avoid potential overflow, so that the maximum runup height can be captured, as per the assumptions in the equation derived.

3.1 Input parameters

The granular flows were composed of an assembly of 30, 000 rigid spherical particles with a uniform diameter of 0.01 m. According to the commonly used values in numerical simulations of granular medium, the material density of each particle is 2630 kg/m^3 and the material shear modulus was set to be 24,000 MPa (Law et al. 2013； Ng et al. 2013). The contact friction angle of discrete elements was set as 31.5°and the coefficient of restitution was set at 0.5. (cf. Song 2016). The interface friction angle was set as 16.6° which is consistent with the value determined by Choi et al. (2016) in laboratory tests. Details of the input parameters are given in Table 1.

3.2 Numerical testing procedures

The numerical study is divided into two stages: a preparation stage and an impact stage. In the preparation stage, all the particles fall freely and deposit randomly under boundary restrictions then a granular flow body with a continuous depth h of 0.05m is prepared right behind the slit-dam. Initial velocities u ranging from 0.38 m/s to 5.7 m/s are uniformly applied to the assembly of particles. Calculating the Froude number by $N_{Fr} = u/\sqrt{ghcos\theta}$, incoming granular flows with Froude numbers ranging from 0.5 to 7.5 are produced. The range of Froude number is consistent with that of reported channelized debris flows, which ranges from 0.5 to 7.6 based on field observations (Hübl et al. 2009; Scheidl et al. 2013; Cui et al. 2015).

In the impact stage, all the sidewall boundary restrictions are removed so the granular flows start to move and impact the slit-dams. The relative post spacings ($R=b/d$) of slit-dams range from 2 to 12, with the transverse blockage (B) between 10 % and 60 % (Silva et al. 2016; Choi et al. 2016). A control test without spacing was also conducted for reference. A summary of the numerical test plans is given in Table 2.

3.3 Model calibration

To ensure that the input parameters and modelling methodology are able to simulate the interaction between granular flows and slit-dams, numerical simulation of the granular flows were compared with experimental results reported by Choi et al. (2016). Fig. 3 shows a comparison of flow kinematics between experimental tests and numerical simulations: the granular flow behaviors of flume tests are shown on the left (Fig .3(a1-a3)) while the pertinent numerical results by DEM are shown on the right (Fig.3(b1-b3)). A wedge-shaped flow front (Choi et al. 2014a) with a Froude number of 2.3 arrives behind the barrier at t = 0.2 s (Fig. 3 (a1) and (b1)); subsequently, particles in the flow front runup along the rigid barrier like water at t = 0.4 s (Fig. 3 (a2) and (b2)); subsequent granular flow impacts and piles up on top of the existing deposits, forming a ramp-like dead zone (Gray et al. 2003) at t = 0.6 s (Fig. 3 (a3) and (b3)); Thereafter, the dead zone continues to thicken and expand upstream until the arrest of granular motion for all particles.

It is observed that the flow kinematics from flume experiments and the calibrated model are consistent. The agreements of the Froude number and flow kinematics between the numerical and experimental results indicate that the set of input parameters and the numerical model used for this study can effectively model the interaction between granular debris flows and slit-dams and the basic mechanisms can be captured.

4. Interpretation of DEM results

4.1 Granular flows runup mechanism

Fig. 4 shows a side view of the impact and runup process of a subcritical flow (N_{Fr} = 0.5) and a supercritical flow (N_{Fr} = 6.5), respectively. At t = 0 s, both subcritical and supercritical flows approach the barrier with an identical flow height (Fig. 4 (a1) and (b1)). For the subcritical flow, a typical pileup mechanism can be observed: the granular bore continues to thicken while the runup height does not change (Choi et al.,

2015b). At t = 0.1 s, the granular flow impacts the slit-dam and most particles in front of the flow deposit behind the rigid barrier, forming a ramp-like dead zone at the base of the barrier while a small number of particles pass through the slit between the posts (Fig. 4 (a2)). As subsequent flow material impacts the existing deposits, the pileup continues to develop, and the dead zone expands upward (Fig. 4 (a3)). Thereafter, the dead zone continues to thicken while maintaining a constant height (Fig.4 (a4) and (a5)). Numerical simulation results indicate that subcritical granular flows exhibit distinct pileup characteristics which are consistent with the experimental observation of Armanini et al. (2011) and Choi et al. (2015b).

Supercritical granular debris flows resulted to a combination of a vertical jet runup and a pileup mechanism. At t = 0 s, a distinct upward jet along the barrier forms as the supercritical flow impacts the slit-dam (Fig. 4 (b2)). Such a runup mechanism is more reminiscent of the vertical jet mechanism described by Armanini et al. (2011) and Choi et al. (2015b) for liquid flows and is consistent with Ng et al. (2017) and Cui et al. (2018) for granular flows of large glass particles. Subsequently, runup continues to develop and the runup height keeps increasing. Simultaneously, a large number of particles pass through the spacing, discharging dispersedly as a downstream jet. (Fig. 4 (b3)). When the maximum runup height is reached, the runup process ceases. Concurrently, the pileup process begins: the dead zone keeps thickening while its height remains unchanged (Fig. 4 (b4)). The numerical simulation results demonstrate that the runup mechanism between subcritical and supercritical granular flows are quite different, subcritical granular flows only exhibit a pileup mechanism while supercritical flows show a combination of vertical jet runup and pileup mechanism.

Fig. 5 shows the evolution of runup heights. In this numerical study, the initial incoming flow is homogeneous, steady and uniform so that the runup height grows without intense fluctuation. Fig. 5(a) shows the time series of runup heights in simulations of different Froude numbers. For the flows with low Froude numbers (e.g. $N_{Fr.}$< 3.5), the runup height rapidly reaches its peak values and then maintains an

almost constant level. For flows with high Froude numbers (e.g. $N_{Fr} > 4.5$), the runup height keeps increasing until the maximum runup height is reached. This increase is non-linear: the growth rate varies in different periods. At first, the runup heights rapidly increases and the growth rate reaches its peak value as the flow front impacts the dam. Thereafter, the growth rate decreases over time, whilst the runup process gradually ceases. After reaching the peak value, the runup heights decrease slowly and then maintain a constant level, indicating that the pileup process is underway. Fig. 5(b) shows the time series of runup heights for different relative post spacings. Numerical simulation results reveal that the evolution of runup heights in different relative post spacings share a similar tendency: the runup height increases over time to a peak value then remains at a constant level. The runup height evidently depends on relative post spacing: the greater the relative post spacing, the lower the maximum runup height and the lesser time it takes to reach it. These results indicate that the slit size affects the runup of granular flows against slit-dams (see later sections).

4.2 Comparison of runup prediction models

Fig. 6 shows the relationship between the transverse blockage B and the normalized outflow velocity $\alpha = u_2/u_0$. The numerical simulation results show that as the transverse blockage B of slit-dams increases, the normalized outflow velocity increases monotonically. Granular debris flows with different Froude conditions (N_{Fr}) all meet with this tendency. This trend is consistent with the assumption we have made in our analytical model (see section 2). By plotting B against α, it is found that the best match can be obtained when the empirical coefficient e is equal to 1.519.

Fig. 7(a) shows the comparison between the simulated normalized runup heights and the analytical approach of Armanini & Larcher (2001). The results illustrate that this approach cannot predict the runup heights of granular flows well: the predictions are too high when the relative post spacing is low but are too conservative when the relative post spacing is high. This is because this approach assumes that runup process

is under the hydraulic jump condition (Armanini & Larcher, 2001), making it inappropriate for frictional dense granular flows, in which the flow-structure interaction mechanism is dominated by pileup (Choi et al. 2016).

It is reported that the momentum approach can capture the runup mechanism of granular flows andcan predict the runup heights well (Choi et al. 2015b; Iverson et al. 2016; Ng et al. 2017). Using the analytical model derived here (see section 2), Fig. 7(b) shows a comparison between the simulated normalized runup heights and the modified momentum approach in this study. The results indicates that this model can indeed predict the runup heights of the granular debris flows against slit-dams quite well. Runup heights predicted by this model show the same tendency with the numerical simulation results: higher Froude number (N_{Fr}) and lower transverse blockage (B) lead to higher runup heights. The maximum error between the predicted runup heights and the numerical results is below 15.6%. According to these results, engineers anticipating a dense granular debris flow can safely use the newly-derived equation to estimate the height required for the slit-dam to avoid dangerous overtopping. Furthermore, the results show the influence of the upstream Froude conditions (N_{Fr}) on runup heights for granular flows against slit-dams. As the Froude number of an incoming flow increases, the maximum runup height increases monotonically, which is consistent with Choi et al. (2015), Iverson et al. (2016) and Ng et al. (2017).

Fig. 8 shows a comparison of the normalized runup height predicted by Armanini & Larcher (2001) and the momentum approach with the reported experimental results (Choi et al. 2016). It is noted that experimental results match well with the runup heights predicted by the momentum approach proposed in this study while the analytical approach of Armanini & Larcher (2001) tends to overestimate, consistent with the DEM numerical results comparisons.

The granular debris flow is composed of an assembly of numerous discrete particles. Therefore, the particle-particle interactions and particle-barrier interactions

362 do significantly affect the flow dynamics and then pose a strong influence on the
363 runup behavior. However, all the analytical prediction models based on continuum
364 hypothesis (Hákonardóttir, 2003; Jóhannesson et al. 2009; Armanini et al. 2011; Kwan
365 2012) fail to consider the particle-particle interactions, which should be taken into
366 consideration in runup height prediction.

367 4.3 Influence of the relative post spacing on runup height

368 Jamming occurs when the flow of grains through a spacing and the size of the
369 outlet is not large enough (Janda et al. 2008). Such a jamming is the response of a
370 system to the applied external stresses by developing mechanical structures that block
371 the flow. In granular materials, these structures are called “arches” (Zuriguel et al.
372 2005). For the case of granular debris flows impacting slit-dams, flow material can
373 jam behind the dam due to the formation of arches when the post spacing is not large
374 enough (Law et al., 2015). Fig. 9(a) shows a typical formation of arches of granular
375 flow behind a slit-dam. As the flow front impacts the slit-dam, granular material is
376 subjected to a reflective dynamic impact force from the barrier. Driven by the applied
377 stress, particles in front of the flow rearrange and the structure of the force chains
378 changes, forming an arch (Terzaghi, 1943). Due to the formation of arches,
379 subsequent granular flow tends to slow down or halt (Arévalo & Zuriguel 2016).
380 Fig. 9(b) shows the evolution of the granular outflow rate for slit-dams with
381 different relative post spacings. It can be seen that outflow rate increases with the
382 relative post spacing since the wider the spacing, the more flow material can pass
383 through. It was found that the evolution of the outflow rate tends to fluctuate
384 periodically, which may be related to the formation of arches. When arches form,
385 granular material blocks the opening and momentarily halts subsequent flow, which
386 leading to a decrease in outflow rate: from a local maximum value to minimum. On
387 the other hand, the outflow rates tend to increase from a local minimum value to the
388 maximum if the arches collapse. It was also found that the formation of arches is

influenced by the slit size. Arches are formed easier at low relative post spacings, at times resulting to near zero outflow rates. As the relative post spacing increases, there are lesser instances at which arches form and the outflow rate can easily reach its minimum level.

In analytical models, the maximum normalized runup height decreases monotonically as the transverse blockage increases (Armanini & Larcher 2001). Such a principle is validated for granular flow problems with a maximum solid volume fraction of 0.01 (Choi et al. 2016). However, for frictional flows such as granular flows, the formation of arches and the interparticle contact should be taken into consideration. When the relative post spacing is small, particles in front of the flow can jam easily behind the slit-dam, blocking the subsequent flow and resulting to a maximum runup height that is usually larger than expected.

Fig. 10 shows the relationship between the normalized maximum runup heights and relative post spacings. The numerical simulation results are compared with experimental data (Choi et al. 2016), which has a similar configuration in channel geometry, granular material property and slit structure type with study while Froude numbers are smaller than 2.3.

For low Froude numbers $(N_{Fr} \leq 2.5)$, the runup heights of the numerical study are very close to the measured values by Choi et al. (2016). The results show that the normalized maximum runup height is not strongly influenced by the relative post spacing. This is because stable arches can easily form at the slit, provided that the Froude number of the incoming flow is low $(N_{Fr} \leq 2.5)$. In this case, there is no significant difference between slit-dams of different slit sizes since the stable arches can block the outlet and halt the flows. When the Froude number is high $(N_{Fr} \geq 2.5)$, supercritical flows with high velocities can break arches easily (Choi et al. 2016). Pardo and Sáez (2014) observed that the arch strength evidently depends on the its length: shorter arches are generally stronger because higher contact stresses can be maintained during constrictions. The length of arches is directly related to the relative

post spacing and the probability of formation of stable arches decreases as *b/d* increases (Janda et al. 2008; Arévalo & Zuriguel 2016; Marchelli et al. 2019). In this case, the relative post spacings affect the runup height significantly. In general, the maximum runup height declines as the ratio *b/d* increases. The results show that there is a critical value of relative post spacing (R_C): within the critical value, the maximum runup height is insensitive (the decrease rate is within 5%) to the relative post spacing; once *b/d* exceeds the critical value, the maximum runup height decreases rapidly as the relative post spacing increases. Such a critical value has been studied in many previous works and it is noted that a fixed value for *Rc* does not exist (Zuriguel et al. 2005; Janda et al. 2008).

As shown in Fig. 10, the numerical results can be interpreted by demarcating two zones. In zone I ($b/d \leq R_C$, shadow area), the runup heights maintain a constant level within a critical range of the relative post spacing. The critical value *Rc* decreases with the increase of N_{Fr} so that Zone I shrinks as the Froude number of incoming flows increases. In zone II ($b/d \geq R_C$, light area), the relative post spacing has a significant effect on the runup height: the maximum runup height decreases rapidly as *b/d* increases. Zone II expands as N_{Fr} increases and eventually spans the full range of the relative post spacing when the Froude number of the flow is high enough. In this case, granular material fails to form stable arches and the runup height decreases monotonically as the relative post spacing increases.

5. Conclusions

An analytical model based on the momentum approach was derived to predict the runup heights of granular debris flows against slit-dams. A numerical study of granular debris flows impacting slit-dams by discrete element method (DEM) was conducted. The numerical results were compared with analytical models and reported experimental data. The influence of the Froude number (N_{Fr}) and relative post spacing (*b/d*) on the runup height were investigated. The conclusions from this study can be

drawn as follows:

(a) An analytical model based on the momentum approach which considers the effect of the flow regime and the post spacing size is proposed. This model can capture the runup mechanism of granular debris flows against slit-dams and predict the runup heights quite well.

(b) The runup mechanisms between subcritical and supercritical granular flows are different: subcritical granular flows result in a typical pileup mechanism, whereas supercritical flows lead to a combination of vertical jet runup and pileup mechanism.

(c) When the Froude number of the incoming flow is low ($N_{Fr} \leq 2.5$), the runup height is not strongly influenced by the relative post spacing. When the Froude number is high ($N_{Fr} > 2.5$), there is a critical value of relative post spacing (R_C): within the critical value, the maximum runup height is insensitive to the relative post spacing; once b/d exceeds the critical value, the maximum runup height decreases as the relative post spacing increases.

The series of numerical simulations by DEM is aimed at investigating the effect of the Froude number (N_{Fr}) and relative post spacing (b/d) on the runup mechanism. By introducing a single-phase model, the effect of fluid in debris flows is not taken into consideration. In the further study, it is worth to explore on the interactions between solid-liquid two-phase debris flows and slit-dams.

Acknowledgments

The authors acknowledge the financial support from the National Natural Science Foundation of China (grant Nos. 11672318, 51809261), the Key Research Program of Frontier Sciences, Chinese Academy of Sciences (CAS) (grant no. QYZDB-SSW-DQC010), and the 135 Strategic Program of the Institute of Mountain Hazards and Environment, CAS (grant no. SDS-135-1701).

References

Albaba A, Lambert S, Faug T (2018). Dry granular avalanche impact force on a rigid wall: Analytic shock solution versus discrete element simulations. Physical Review E, 97(5), 052903

Arévalo R, Zuriguel I (2016) Clogging of granular materials in silos: effect of gravity and outlet size. Soft Matter 12(1):123-130

Armanini A, Larcher M (2001) Rational criterion for designing spacing of slit-check dam. Journal of Hydraulic Engineering 127(2):94-104

Armanini A, Larcher M, Odorizzi M (2011) Dynamic impact of a debris flow front against a vertical wall. In Proceedings of the 5th International Conference on Debris-Flow Hazards Mitigation: Mechanics, Prediction and Assessment, pp. 1041-1049 Padua, Italy

Chau K, Wong RHC, Wu JJ (2002) Coefficient of restitution and rotational motions of rockfall impacts. International Journal of Rock Mechanics and Mining Sciences 39(1):69-77

Chen HX, Li J, Feng S J, Gao H Y, Zhang DM (2019). Simulation of interactions between debris flow and check dams on three-dimensional terrain. Engineering Geology, 251, 48-62.

Choi CE, Ng CWW, Song D, Kwan JHS, Shiu HYK, Ho KKS, Koo RCH (2014a) Flume investigation of landslide debris–resisting baffles. Canadian Geotechnical Journal 51(5):540-553

Choi CE, Ng CWW, Law RP, Song D, Kwan, JSH, Ho KKS (2014b) Computational investigation of baffle configuration on impedance of channelized debris flow. Canadian Geotechnical Journal 52(2):182-197

Choi CE, Ng CWW, Au-Yeung SCH, Goodwin GR (2015a) Froude characteristics of both dense granular and water flows in flume modelling. Landslides 12(6):1197-1206

Choi CE, Au-Yeung SCH, Ng CWW, Song D(2015b) Flume investigation of landslide granular debris and water runup mechanisms. Géotechnique Letters 5(1):28-32

Choi CE, Goodwin GR, Ng CWW, Cheung DKH, Kwan JS, Pun WK (2016) Coarse granular flow interaction with slit structures. Géotechnique Letters 6(4):267-274

Chu T, Hill G, McClung DM, Ngun R, Sherkat R (1995) Experiments on granular flows to predict avalanche runup. Canadian Geotechnical Journal 32(2):285-295

Cui P, Zeng C, Lei Y (2015) Experimental analysis on the impact force of viscous debris flow. Earth Surface Processes and Landforms 40(12):1644-1655

Cui Y, Choi CE. Liu LH, Ng CWW (2018) Effects of particle size of mono-disperse granular flows impacting a rigid barrier. Natural Hazards, 91(3), 1179-1201

Cundall PA, Strack OD (1979) A discrete numerical model for granular assemblies. Geotechnique 29(1):47-65

Denlinger RP, Iverson RM (2001) Flow of variably fluidized granular masses across three-dimensional terrain: 2. Numerical predictions and experimental tests. Journal of Geophysical Research: Solid Earth 106(B1):553-566

Faug T (2015) Depth-averaged analytic solutions for free-surface granular flows impacting rigid walls down inclines. Physical Review E, 92(6), 062310

Gray JMNT, Tai YC, Noelle S (2003) Shock waves, dead zones and particle-free regions in rapid granular free-surface flows. Journal of Fluid Mechanics 491:161-181

Hákonardóttir KM (2003) A laboratory study of the interaction between supercritical, shallow flows and dams. Icelandic Meteorological Office (Vedurstofa Islands) Report 03038

Hübl J, Suda J, Proske D, Kaitna R, Scheidl C (2009) Debris flow impact estimation. In Proceedings of the 11th international symposium on water management and hydraulic engineering, Ohrid, Macedonia pp.1-5

Hungr O, Morgan GC, Kellerhals R (1984) Quantitative analysis of debris torrent hazards for design of remedial measures. Canadian Geotechnical Journal 21(4):

663-677

Hungr O, McClung DM (1987) An equation for calculating snow avalanche runup against barriers. National Research Council Canada, Institute for Research in Construction

Iverson RM (1997) The physics of debris flows. Reviews of geophysics 35(3):245-296

Iverson RM, Denlinger RP (2001) Flow of variably fluidized granular masses across three-dimensional terrain: 1. Coulomb mixture theory. Journal of Geophysical Research: Solid Earth, 106(B1), 537-552

Iverson RM, George DL, Logan M (2016) Debris flow runup on vertical barriers and adverse slopes. Journal of Geophysical Research: Earth Surface 121(12):2333-2357

Jakob M, Hungr O, Jakob DM (2005) Debris-flow hazards and related phenomena Vol. 739, Berlin: Springer

Janda A, Zuriguel I, Garcimartín A, Pugnaloni LA, Maza D (2008) Jamming and critical outlet size in the discharge of a two-dimensional silo. EPL (Europhysics Letters) 84(4):44002

Jóhannesson T, Gauer P, Issler P, Lied K, Hákonardóttir KM (2009) The design of avalanche protection dams: recent practical and theoretical developments

Kwan JSH (2012) Supplementary technical guidance on design of rigid debris-resisting barriers. Geotechnical Engineering Office, HKSAR. GEO Report (270)

Lambe, T.W., and R.V. Whitman (1979), Soil Mechanics, SI Version, Wiley, New York.

Law RPH, Choi CE, Ng CWW (2015) Discrete-element investigation of influence of granular debris flow baffles on rigid barrier impact. Canadian Geotechnical Journal 53(1):179-185

Mancarella D, Hungr O (2010) Analysis of runup of granular avalanches against steep,

553 adverse slopes and protective barriers. Canadian Geotechnical Journal
554 47(8):827-841
555 Marchelli M, Leonardi A, Pirulli M, Scavia C (2019) On the efficiency of slit-check
556 dams in retaining granular flows. Géotechnique 1-39
557 Ng CWW, Choi CE, Law RP (2013) Longitudinal spreading of granular flow in
558 trapezoidal channels. Geomorphology: 194 84-93
559 Ng CWW, Song D, Choi CE, Liu LHD, Kwan JSH, Koo RCH, Pun WK (2016)
560 Impact mechanisms of granular and viscous flows on rigid and flexible barriers.
561 Canadian Geotechnical Journal 54(2):188-206
562 Ng CWW, Choi CE, Liu LHD, Wang Y, Song D, Yang N (2017) Influence of particle
563 size on the mechanism of dry granular runup on a rigid barrier. Géotechnique
564 Letters 7(1):79-89
565 Pardo GS, Sáez E (2014) Experimental and numerical study of arching soil effect in
566 coarse sand. Computers and Geotechnics 57:75-84
567 Piton G, Recking A (2015a) Design of sediment traps with open check dams. I:
568 Hydraulic and deposition processes. Journal of Hydraulic Engineering
569 142(2):04015045
570 Piton G, Recking A (2015b) Design of sediment traps with open check dams. II:
571 Woody debris. Journal of Hydraulic Engineering 142(2):04015046
572 Rapaport DC, Rapaport DCR (2004) The art of molecular dynamics simulation.
573 Cambridge university press
574 Scheidl C, Chiari M, Kaitna R, Müllegger M, Krawtschuk A, Zimmermann T, Proske
575 D (2013) Analysing debris-flow impact models, based on a small scale modelling
576 approach. Surveys in Geophysics 34(1):121-140
577 Shen W, Zhao T, Zhao J, Dai F, Zhou GG (2018) Quantifying the impact of dry debris
578 flow against a rigid barrier by DEM analyses. Engineering Geology 241:86-96
579 Song D (2016) Mechanisms of debris flow impact on rigid and flexible barriers
580 (Doctoral dissertation)

581 Terzaghi K (1943) Arching in ideal soils. In Theoretical Soil Mechanics. Hoboken, NJ,
582 USA: Wiley
583 TranscenData Europe Limited (2006) Version 2.6.0
584 Zhou GG, Sun QC (2013) Three-dimensional numerical study on flow regimes of dry
585 granular flows by DEM. Powder technology 239:115-127
586 Zhou GG, Hu HS, Song D, Zhao T, Chen XQ (2019) Experimental study on the
587 regulation function of slit dam against debris flows. Landslides:1-16
588 Zuriguel I, Garcimartín A, Maza D, Pugnaloni LA, Pastor JM (2005) Jamming during
589 the discharge of granular matter from a silo. Physical Review E 71(5):051303

List of figures

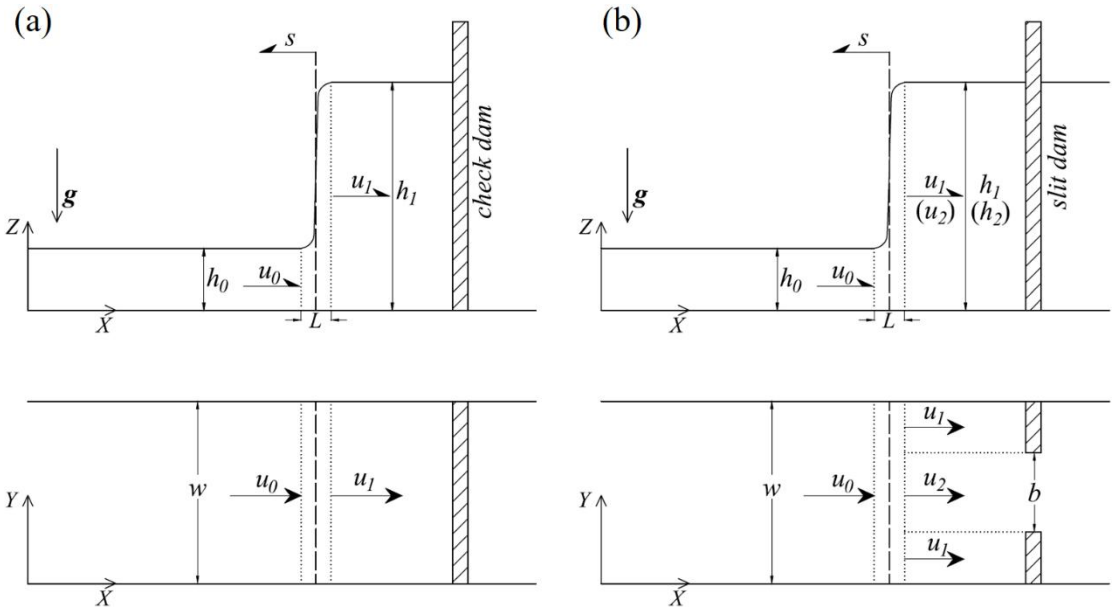

Fig. 1. Schematic drawing (side view and plan view) of runup against (a) a check dam and (b) a slit-dam.

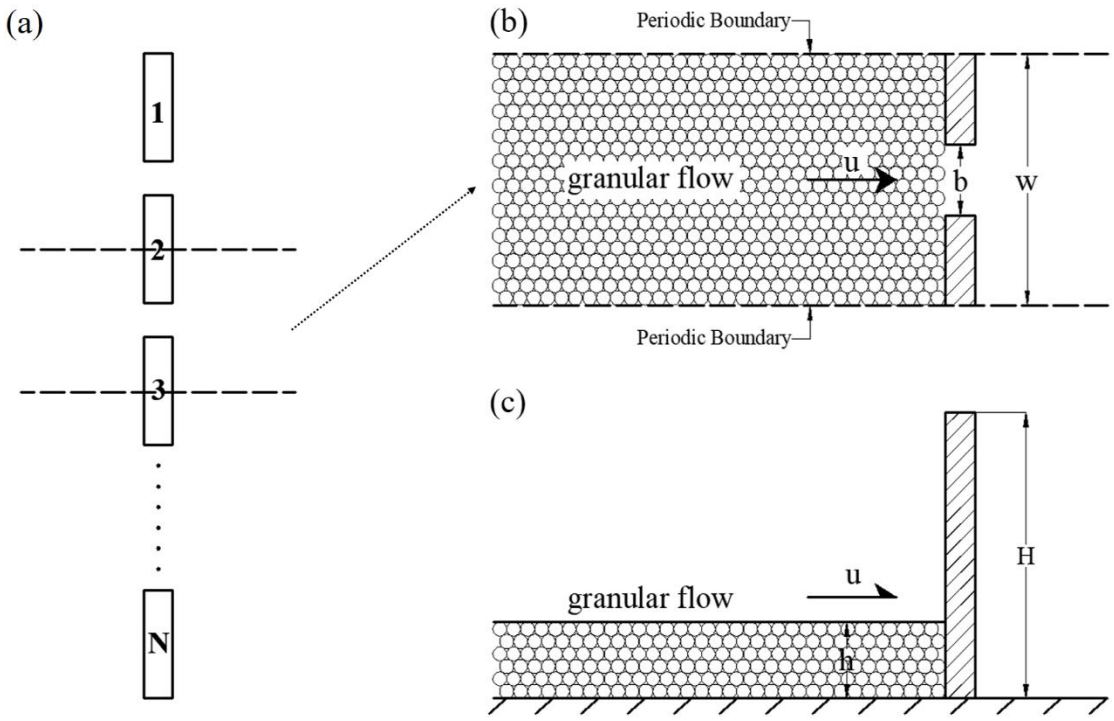

Fig. 2. Numerical model: (a) a chosen section of slit-dam; (b) plan view of the chosen section; (c) side view of the chosen section

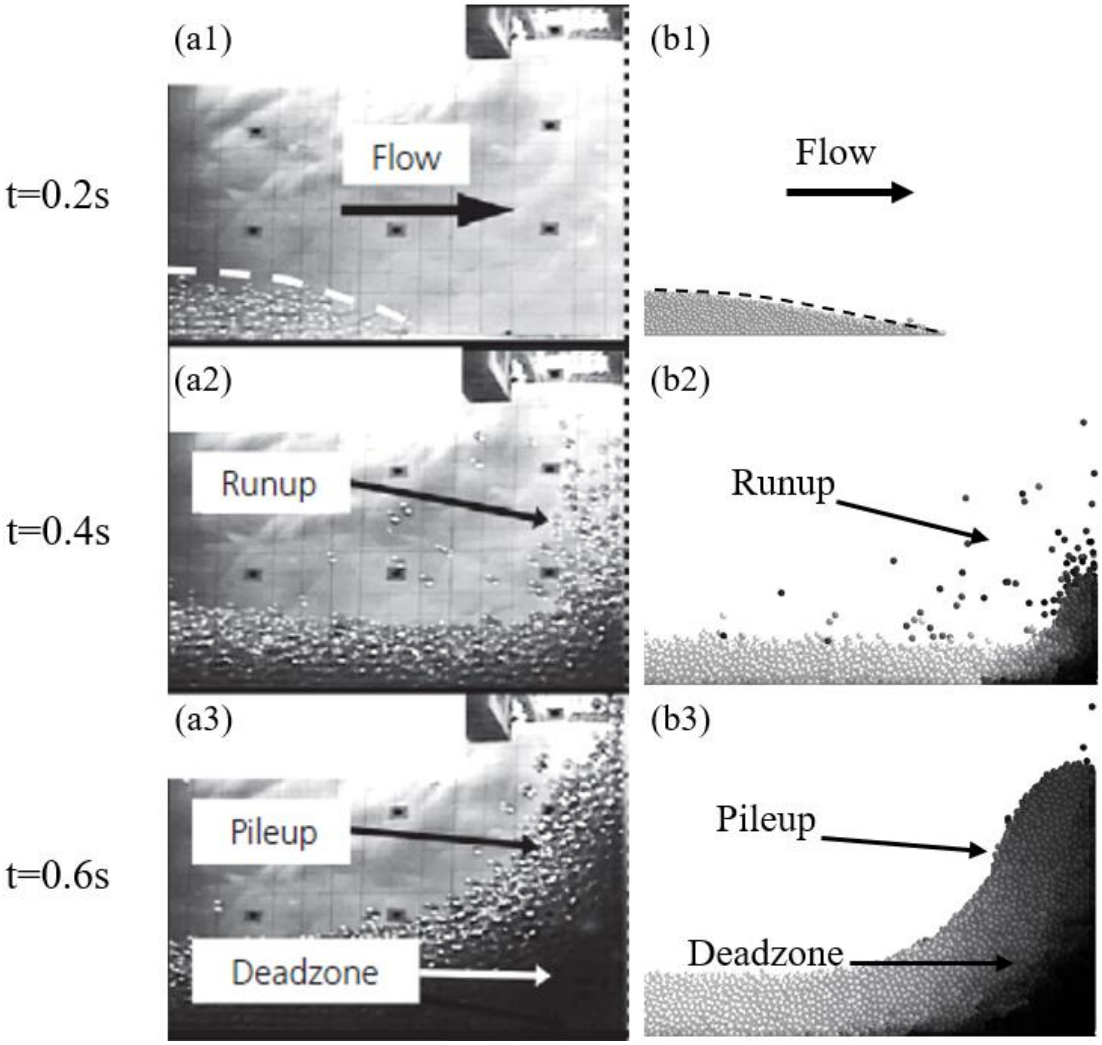

Fig. 3. Comparison of flume experiments and computed flow kinematics (test C30-D1-SD5, wherein inclination = 30° , b/d = 5.0) . The color of particles denotes the velocity of particles and the darker the color, the lower the velocity.

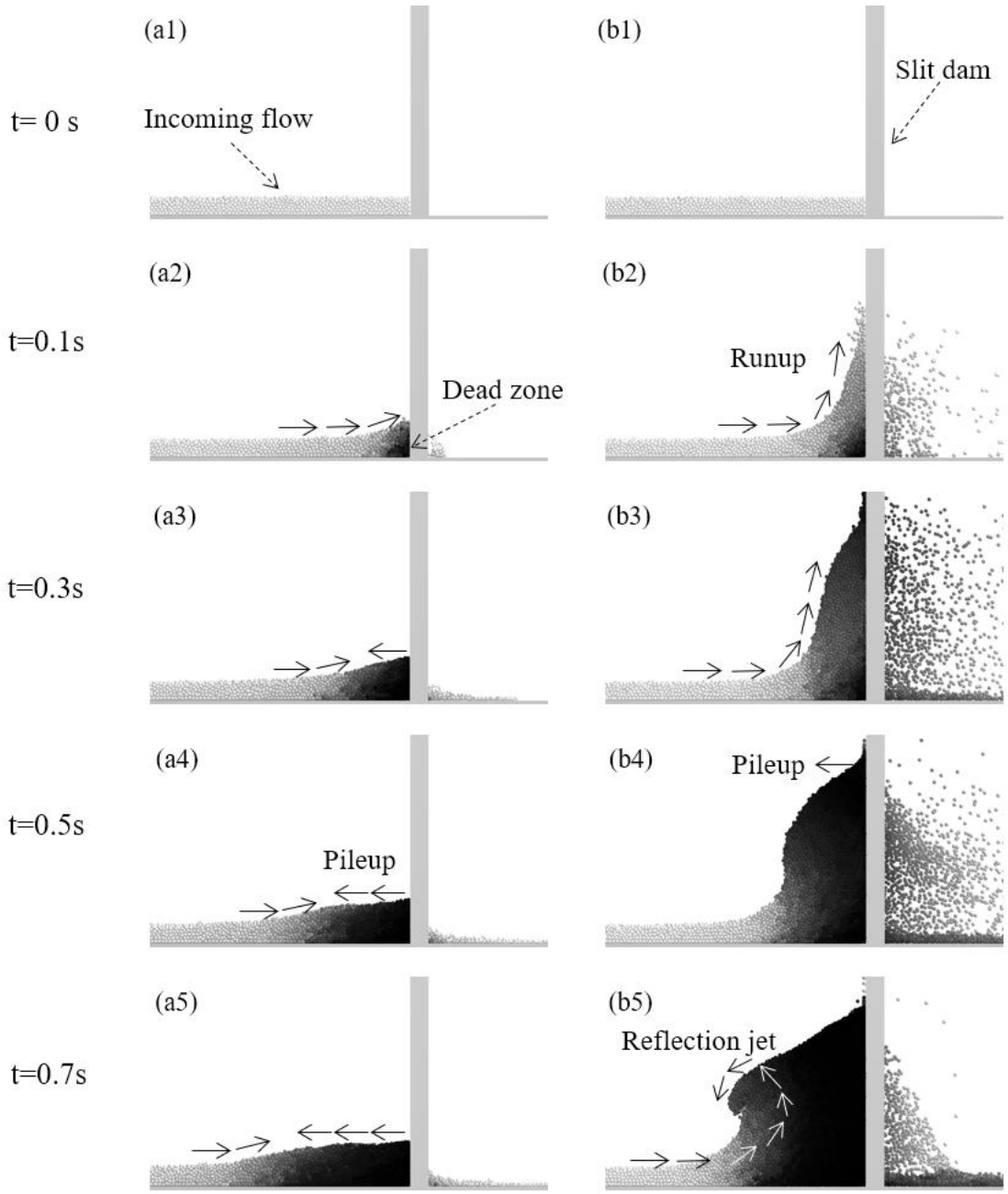

Fig. 4. Simulated flow kinematics for subcritical flow (N_{Fr} = 0.5) (a1-a5) and supercritical flow (N_{Fr} = 6.5) (b1-b5), b/d = 2.0. The color of particles denotes the velocity of particles and the darker the color, the lower the velocity.

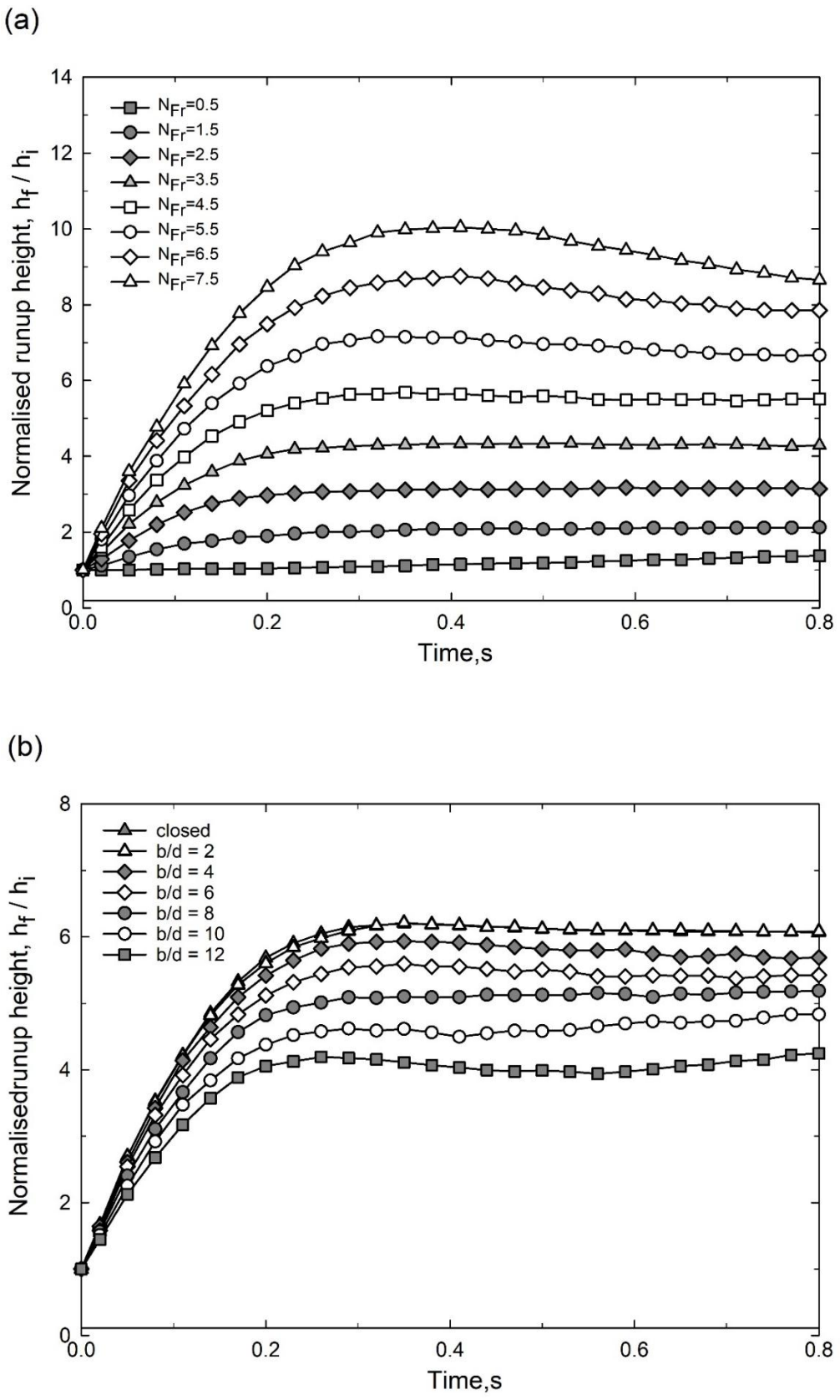

Fig. 5. Evolution of the runup height. (a) b/d = 4.0, (b) N_{Fr} = 4.5, where zero time corresponds to the time instance at which the flow front reaches the dam.

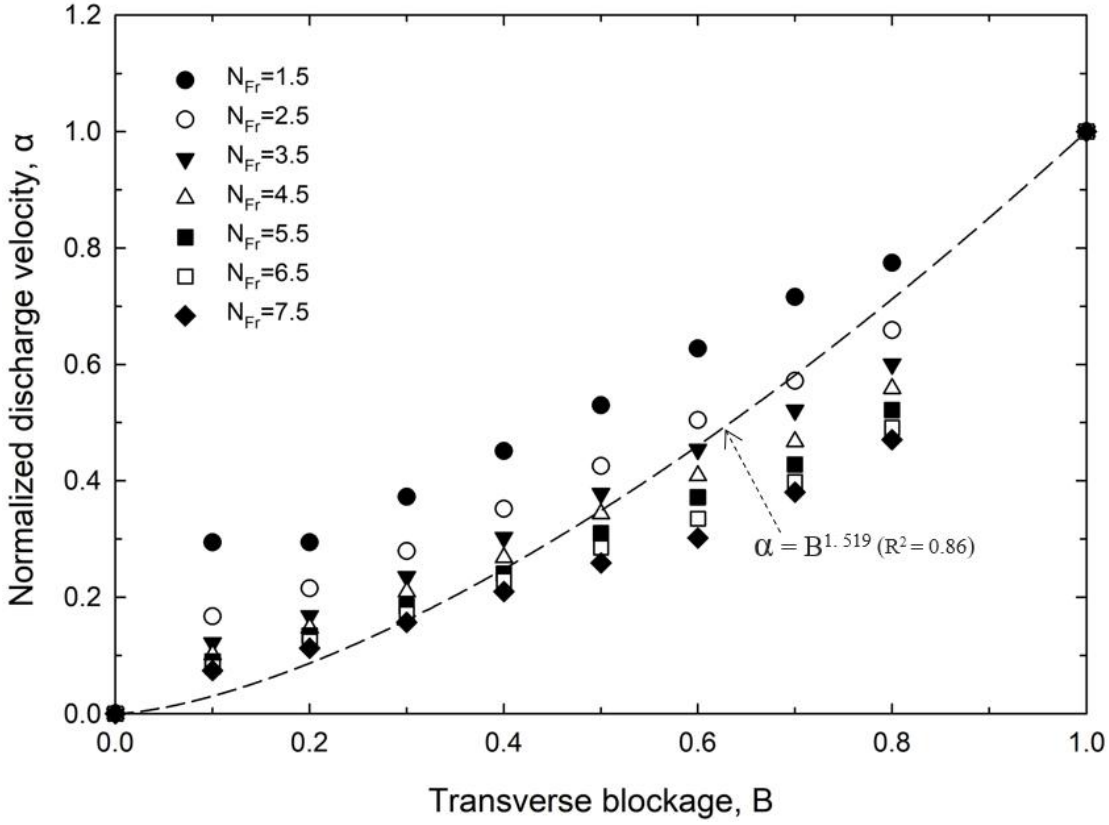

Fig. 6. Relationship between transverse blockage and normalized outflow velocity.

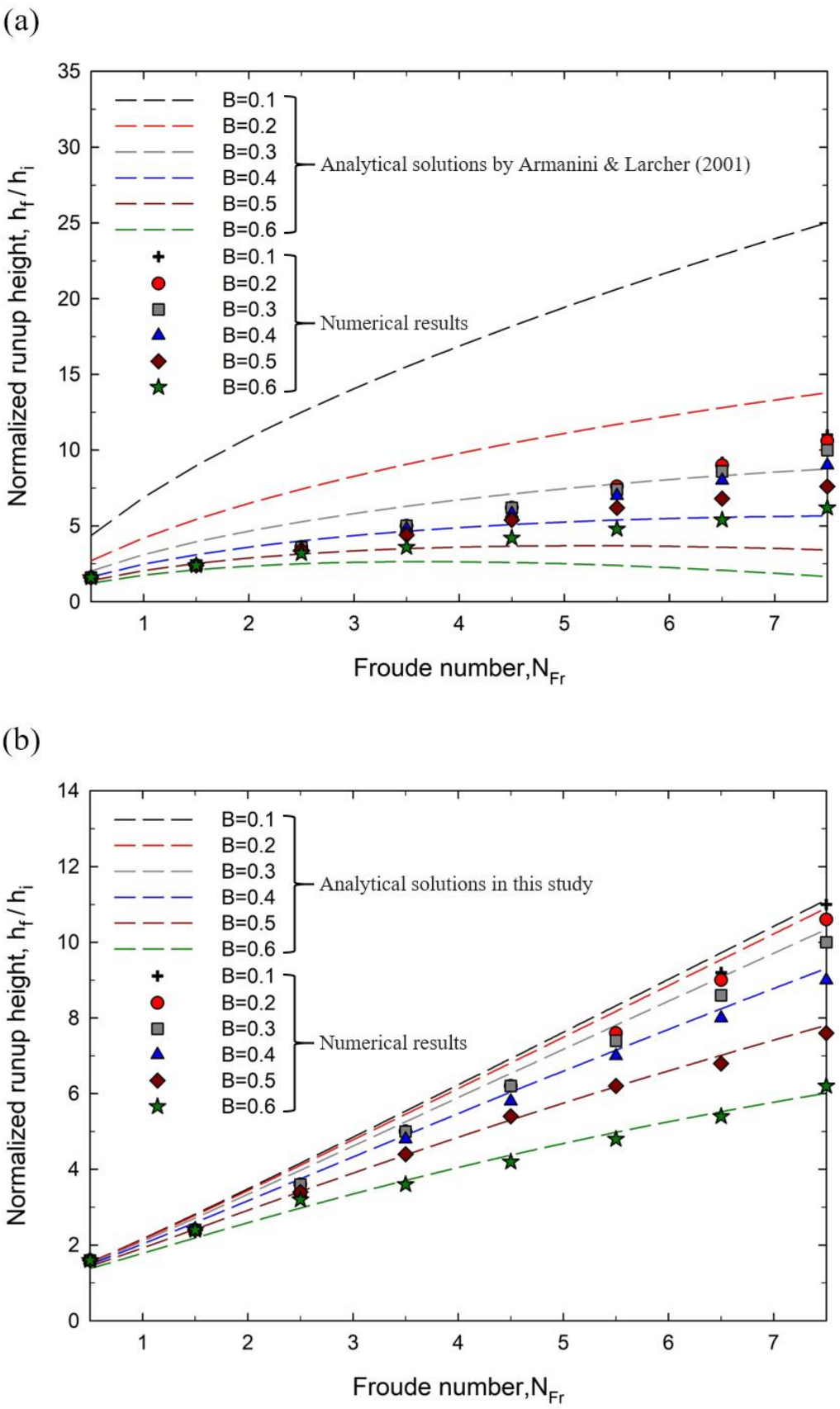

Fig. 7. Comparison of theoretical normalised runup height predicted by (a) the energy approach and (b) the momentum approach ($\boldsymbol{e}$ =1.519) with the DEM results.

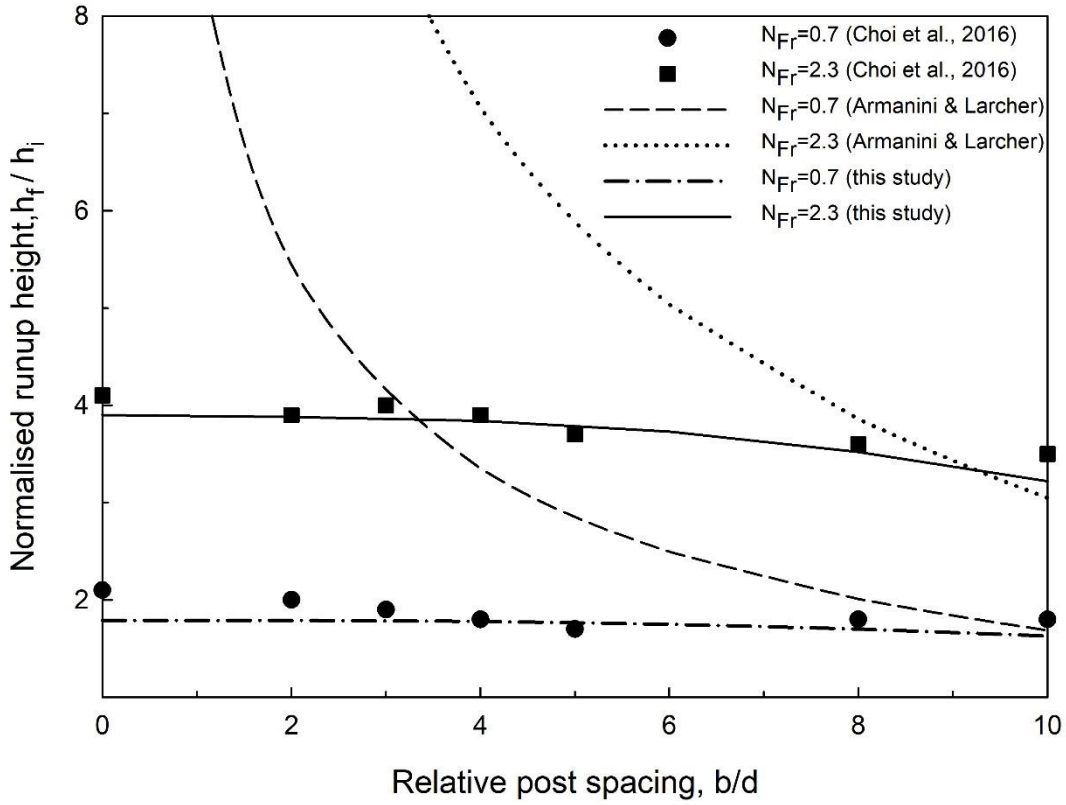

Fig. 8. Comparison of theoretical normalised runup height predicted by the energy approach and the momentum approach (e = 1.519) with the reported experimental results.

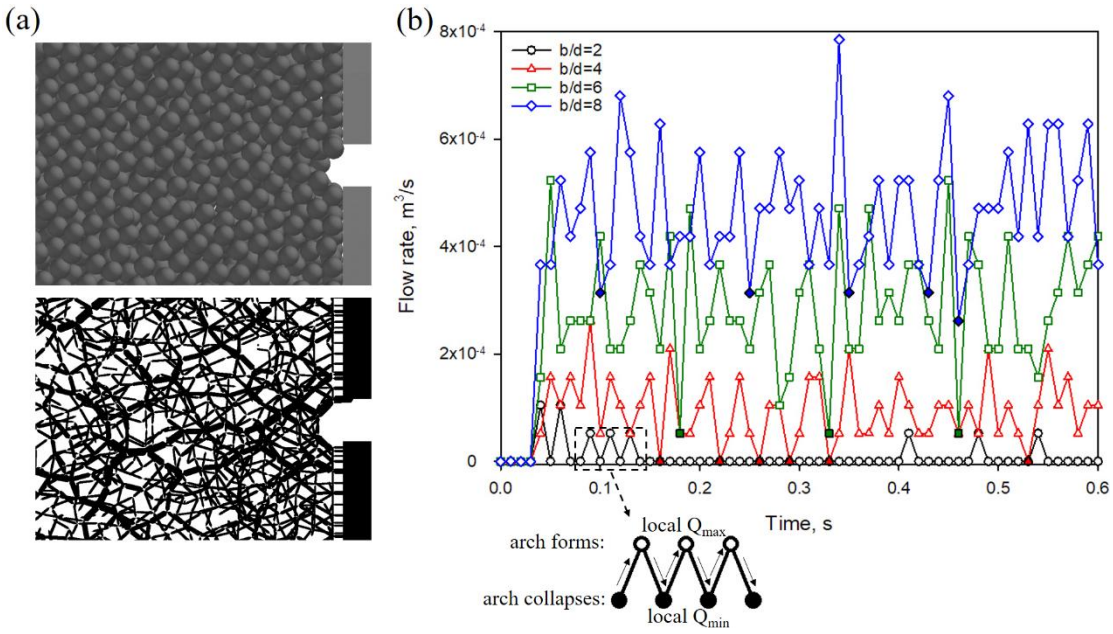

Fig. 9. (a) arches and force chains in granular flow behind a slit-dam (N_{Fr} = 0.5;b/d = 2.0); (b) evolution of the granular outflow rate for slit-dams with different relative post spacing b/d (solid point denotes the local Q_{min}).

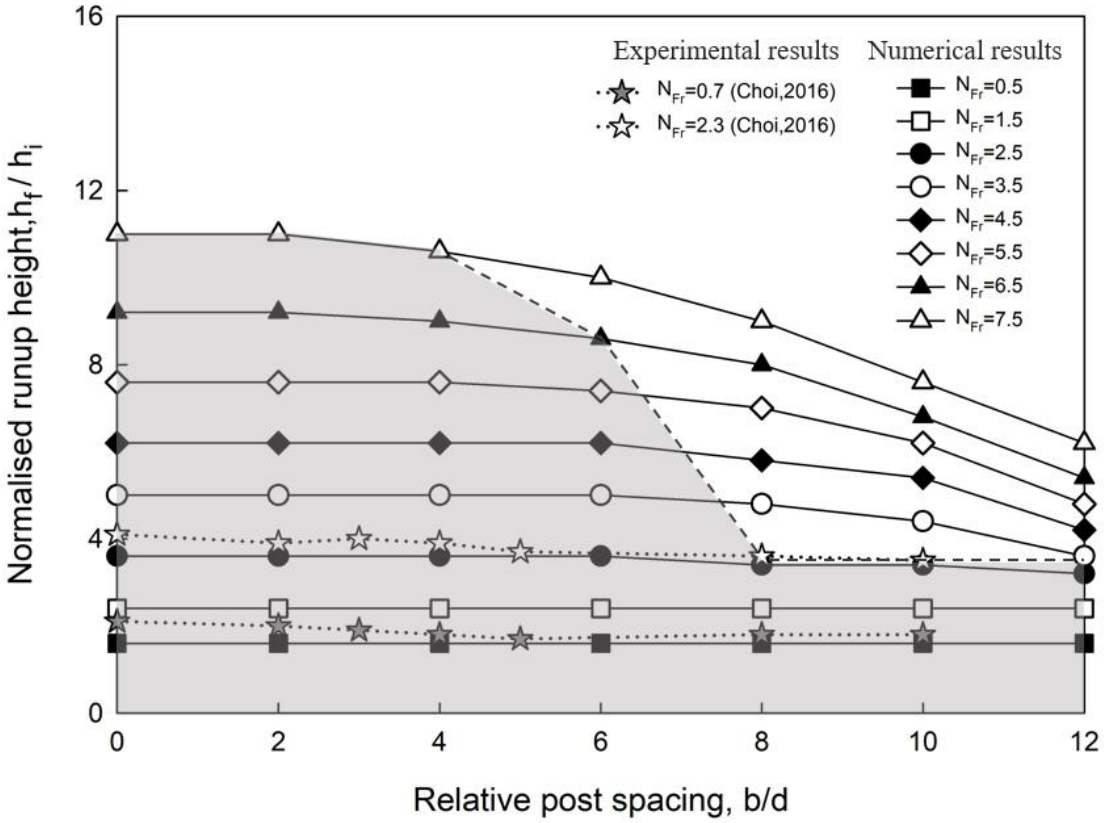

Fig. 10. Relationship between runup height and relative post spacing.

Table 1. DEM input parameters.

Input parameter	Value
Number of discrete elements	50,000
Particle diameter (m)	0.01
Density (kg/m^3)	2630
Total mass of particles (kg)	68.85
Shear Modulus (MPa)	24000
Discrete element/wall friction	0.3
Discrete element friction	0.6
Rolling friction coefficient	0.01
Coefficient of restitution	0.5

Table 2. Numerical simulation plan.

Relative post spacing ($R=b/d$)	Transverse blockage ($B=b/w$)	Initial Froude condition (N_{Fr})
0	0%	
2	10%	
4	20%	0.5；1.5；2.5；
6	30%	3.5；4.5；5.5;
8	40%	6.5；7.5
10	50%	
12	60%	